

# Foot Placement in the Simplest Slope Walker Reveals a Wide Range of Walking Solutions

Pranav A. Bhounsule

**Abstract**—We show that the simplest slope walker can walk over wide combinations of step lengths and step velocities at a given ramp slope by proper choice of foot placement. We are able to find walking solutions up to slope of 15.42 degrees, beyond which the ground reaction force on the stance leg goes to zero, implying a flight phase. We also show that the simplest walker can walk at human sized step length and step velocity at a slope of 6.62 degrees. The central idea behind control using foot placement is to balance the potential energy gained during descent with the energy lost during collision at foot-strike. Finally, we give some suggestions on how the ideas from foot placement control and energy balance can be extended to realize walking motions on practical legged systems.

**Index Terms**—simplest walker, passive dynamic walking, foot placement, compass gait, Poincaré map.

## I. INTRODUCTION

There is a class of robots, called passive dynamic walkers, that can walk down shallow inclines without any control or energy input. Passive dynamic walkers were first demonstrated in experiment by McGeer[1]. Further, he used tools in dynamical systems; namely, Poincaré return map to search for walking gaits and eigenvalues of the linearized return map to explain stability of the walking motions.

McGeer found that the robot morphology like mass, inertia, leg length, foot radius, and the ramp slope influence the dynamics of the walking gait. A better insight into the mechanics of passive dynamic walkers might be achieved by reducing the parameter space. In this spirit, Garcia et al. [2] did an extreme simplification to the passive dynamic walking model analyzed by McGeer. They put a point mass at the hip and infinitesimal point mass at each foot of the straight leg walker. After non-dimensionalizing the equations of motion, they demonstrated that the model has only one free parameter, the ramp slope.

The model analyzed by Garcia et al., called the simplest walker, demonstrates two families of period-one walking solutions (a walking motion that repeats itself every step); a stable solution and an unstable solution. There is one stable period-one solution for each slope in the range 0 to 0.87 degrees. As the slope is increased beyond 0.87 degrees, higher period walking emerges, ultimately leading to chaotic walking. There are no stable passive walking solutions for the simplest walker beyond a slope of 1.1 degrees. On the other hand, there is one unstable period-one solution for each slope in the range 0 to 15.42 degrees. Beyond 15.42 degrees there are no walking solutions because the ground reaction force on the stance leg goes to zero.

In this paper, we explore the range of walking solutions for the hip actuated simplest walker. In particular, we use the hip actuator to do accurate foot placement. Using foot placement for control of legged systems is not new. Pratt et al. [3] defined the capture point as the location where the robot needs to place its foot to come to a complete stop when pushed. They computed the capture point based on the zero of the orbital energy of the robot idealized as a linear inverted pendulum with smooth support transfer.

Wight et al. [4] introduced the concept of foot placement estimator, which is identical to the capture point concept. However, unlike Pratt

et. al, they used the inverted pendulum model with collisional support transfer which is similar to the model used here. We will analysis similar to that of Pratt et al. and Wight et al. but to compute the feasible walking solutions for the simplest slope walker [2].

In this paper, by means of theoretical calculations we demonstrate that: (1) By controlling foot placement in the simplest walker, and a suitable choice of slope, wide combinations of speeds and step lengths are possible. (2) A feed-forward control law that achieves a particular foot placement strategy can be numerically computed. (3) Walking at average human speed and stride length is possible by appropriate choice of slope.

## II. BIPED MODEL

### A. Model description

Fig. 1 (a) shows a cartoon of the simplest walker. The model has a mass  $M$  at the hip and point mass  $m$  at each of the feet. Each leg has length  $\ell$ , gravity  $g$  points downwards, and the ramp slope is  $\gamma$ . The leg in contact with the ramp is called the stance leg while the other leg is called the swing leg. The angle made by the stance leg with the normal to the ramp is  $\theta$  and the angle made by the swing leg with the stance leg is  $\phi$ . The hip torque is  $U$ . Fig. 1 (b) describes a typical step of the simplest walker. The walker starts in (i), the state in which the front leg is the stance leg and the trailing leg is the swing leg. The walker moves from (ii) to (v) as shown. We ignore foot scuffing. Finally in (vi), the swing leg collides with the ground and becomes the new stance leg. At this point, we have a complete gait cycle with the state configuration (vi) being the same as (i).

### B. Equations of motion

The equations of motion for the simplest walker are given in Garcia et al. [2]. The only addition we make is the introduction of a non-dimensional hip torque  $u$ . We give a brief overview on the derivation of the equations of motion. The reader who is familiar with the equations of motion can skip to the next section.

The equations of motion consist of two phases and one event and are described below.

- **Single stance phase (continuous dynamics):** In this phase of motion, the stance leg pivots and rotates about the stationary foot; while the swing leg pivots and rotates about the hinge connecting the two legs. We assume that the stance leg does not slip, there is no hip hinge friction, and ignore foot scuffing. We obtain (1) and (2) defined below by taking moments about stance foot contact point and hip hinge respectively, and non-dimensionalizing time with  $\sqrt{\ell/g}$  and applying the limit,  $m/M \rightarrow 0$ . In (2),  $u$  is the non-dimensional torque obtained by dividing the torque,  $U$ , by  $Mg\ell$ . The equations are;

$$\ddot{\theta} = \sin(\theta - \gamma), \quad (1)$$

$$\ddot{\phi} = \sin(\theta - \gamma) + \{\dot{\theta}^2 - \cos(\theta - \gamma)\} \sin(\phi) + u. \quad (2)$$

- **Foot-strike event:** We integrate the single stance equations given above till the foot-strike event, wherein the swing leg is about to impact the ground. Using super-script  $-$  and  $+$  to denote the instance just before and just after foot-strike respectively, we can write the foot-strike event as

$$\phi^- = 2\theta^-. \quad (3)$$

- **Support exchange phase (discontinuous dynamics):** In this phase of motion, the legs exchange their roles, that is, the current swing leg becomes the new stance leg and the current stance leg becomes the new swing leg. We assume that the swing leg has a plastic collision (no slip and no bounce) with the ground,

P. A. Bhounsule is affiliated with Disney Research Pittsburgh, 4720 Forbes Avenue, Lower Level, Suite 110, Pittsburgh, PA, 15213 USA and with the Dept. of Mechanical Engineering, University of Texas San Antonio, One UTSA Circle, San Antonio, TX 78249 USA. e-mail: pab47@disneyresearch.com

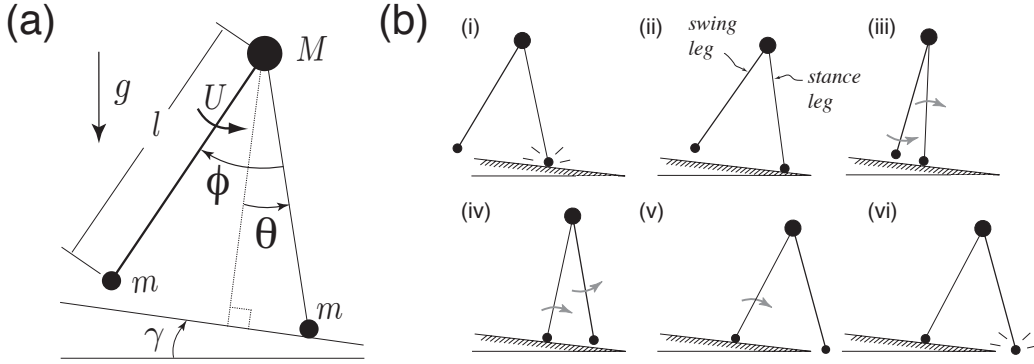


Fig. 1. (a) The simplest walker first analyzed by Garcia et al. [2]. We have added a hip actuator to the model. (b) A typical step of the simplest walker.

is instantaneous, and there is no double support phase. The swapping of legs is expressed by (4) and (6). The angular rates of the legs after support exchange are given by (5) and (7) and are obtained by applying conservation of angular momentum about stance foot contact point and hip hinge respectively, followed by non-dimensionalizing time with  $\sqrt{\ell/g}$  and applying the limit,  $m/M \rightarrow 0$ .

$$\theta^+ = -\theta^-, \quad (4)$$

$$\dot{\theta}^+ = \cos(2\theta^-)\dot{\theta}^-, \quad (5)$$

$$\phi^+ = -\phi^- = -2\theta^-, \quad (6)$$

$$\dot{\phi}^+ = \{1 - \cos(2\theta^-)\} \cos(2\theta^-)\dot{\theta}^-. \quad (7)$$

### III. METHODS

#### A. Analysis using Poincaré return map

We use a Poincaré return map to generate steady state walking motions [1], [2], [5]. Let  $\mathbf{q}_0 = \{\theta_0^+, \dot{\theta}_0^+, \phi_0^+, \dot{\phi}_0^+\}$  be the state after foot-strike and  $u_0(t)$  be the feed-forward control.

We define the function  $\mathcal{S}$  that takes the initial condition,  $\mathbf{q}_0$ , and control,  $u_0$ , and returns the state after one step,  $\mathbf{q}_1$ . Thus, we have the map,  $\mathbf{q}_1 = \mathcal{S}(\mathbf{q}_0, u_0)$ .  $\mathcal{S}$  can be computed numerically by first integrating the equation of motion in the single stance phase (see (1) and (2)) till the foot-strike event (see (3)), and applying the leg support exchange conditions (see (4)-(7)). To generate period-one walking, we need to find the initial conditions such that,

$$\mathbf{q}_0 = \mathcal{S}(\mathbf{q}_0, u_0). \quad (8)$$

To generate period two walking we would need to apply the map  $\mathcal{S}$  twice, and so on. In this paper, we will focus only on period-one walking motions described by (8).

#### B. Passive Dynamic Walking

To generate passive dynamic walking, we put  $u_0 = 0$  and search for four initial conditions defined in  $\mathbf{q}_0$  that would give,  $\mathbf{q}_0 = \mathcal{S}(\mathbf{q}_0, 0)$ . Because of the simplicity of the walker, we can reduce the number of initial condition to be searched as follows. From (3), (6) and (7), we see that only two out of the four initial conditions in  $\mathbf{q}_0$ , say  $\theta^+$  and  $\dot{\theta}^+$ , are independent.

Thus we need to search for only two initial conditions,  $\mathbf{q}_0 = \{\theta_0^+, \dot{\theta}_0^+\}$ . This reduces the Poincaré map,  $\mathcal{S}$ , from four to two dimensions.

#### C. Control of foot placement

In the last section we showed that the Poincaré map can be reduced from four to two dimensions using the special nature of the equations of motion of the simplest walker. Next, we show how our foot placement control law will help us to further reduce the Poincaré map from two to one dimension. Due to the nature of our foot placement law, we will be able to compute the map  $\mathcal{S}$  analytically without the need to integrate the equations of motion. We present the foot placement control next.

We position the swing leg before foot-strike ( $\phi^-$ ) to the angle  $-\phi_0$  (say). That is,

$$\phi^- = -\phi_0. \quad (9)$$

We can now find the position of the stance leg after foot-strike,

$$\theta^+ = -\theta^- = -0.5\phi^- = 0.5\phi_0 = \theta_0 \text{ (say)}. \quad (10)$$

In the above expression, the first, second and third equalities come from (4), (3) and (9) respectively.

From (10), we determine the angle of the stance leg after foot-strike,  $\theta_0$ , by the foot placement control,  $\phi_0$ . Since we specify one of the two initial states (see Section III-B) after foot-strike, the Poincaré map gets reduced from two dimensions to just one dimension, that is,  $\dot{\theta}_0 = \mathcal{S}(\dot{\theta}_0)$ .

Using conservation of total energy between steps, we can compute the period-one walking solution. We multiply (1) with  $\dot{\theta}$  and integrate with respect to time to get a conserved quantity  $E$ .  $E$  is the non-dimensional mechanical energy of the stance leg taken alone during the single stance phase. Thus,

$$E = \frac{\dot{\theta}^2}{2} + \cos(\theta - \gamma) = \text{constant}. \quad (11)$$

For periodic motion,  $E$  will be a constant. Applying (11) to instance before and after foot-strike we get,

$$E^+ = E^-, \quad \frac{(\dot{\theta}^+)^2}{2} + \cos(\theta^+ - \gamma) = \frac{(\dot{\theta}^-)^2}{2} + \cos(\theta^- - \gamma). \quad (12)$$

Let  $\dot{\theta}^+ = \dot{\theta}_0$ . From (10), we have,  $\theta^- = -\theta^+ = -\theta_0$  and from (5), we have,  $\dot{\theta}^- = \sec(2\theta^-)\dot{\theta}^+ = \sec(2\theta_0)\dot{\theta}_0$ . Putting these values in (12) and solving for  $\dot{\theta}_0$  gives,

$$\dot{\theta}_0 = -\cot(2\theta_0)\sqrt{2\{\cos(\theta_0 - \gamma) - \cos(\theta_0 + \gamma)\}}. \quad (13)$$

Note that we have used the negative sign in the expression above as clockwise rotation is negative (see Fig. 1 (a)).

For a given  $\gamma$ , (13) states the relation between the stance leg angle at foot-strike  $\theta_0$  and the stance leg velocity after foot-strike  $\dot{\theta}_0$  for a

period-one walking gait. We can choose one and solve for the other. However, we need to check two conditions that ensure feasibility of walking.

1) *Walking too fast leads to flight phase:* Physics dictates that the stance leg can only push against the ground, and not pull against it. By our sign convention, this implies a positive vertical reaction force between the stance leg and the ground. Thus, if the non-dimensional reaction force on the stance leg from the ground is denoted by  $F$  (non-dimensionalised by  $Mg$ ) then,

$$F = \cos(\theta - \gamma) - \dot{\theta}^2 > 0 \quad \Rightarrow \quad \dot{\theta}^2 < \cos(\theta - \gamma). \quad (14)$$

Equation (14) is most likely to be violated when cosine term has minimum value or when stance leg angle,  $\theta$ , has maximum value. The most extreme angle for a given step length occurs at the instance just before foot-strike. Note that the stance leg angle is negative at the instance before foot-strike. Thus, we need to check the condition,  $(\dot{\theta}^-)^2 < \cos(\theta^- - \gamma)$ . Putting  $\theta^- = -\theta^+ = -\theta_0$  and  $\dot{\theta}^- = \sec(2\theta^-)\dot{\theta}^+ = \sec(2\theta_0)\dot{\theta}_0$ , we get,

$$(\dot{\theta}_0)^2 < \cos^2(2\theta_0) \cos(\theta_0 + \gamma). \quad (15)$$

2) *Walking too slow leads to falling backwards:* We need to rule out angular velocities,  $\dot{\theta}^+$ , that are too slow and will not make it to the top of the pendulum arc of the stance leg. In this case, the robot will fall backwards.

The angular velocity at mid-stance  $\dot{\theta}^m$  (instance when the stance leg is parallel to the gravity vector) can be computed by doing an energy balance between the instance after foot-strike and mid-stance position (see (11)) to get

$$\begin{aligned} \dot{\theta}^m &= -\sqrt{(\dot{\theta}^+)^2 + 2\cos(\theta^+ - \gamma) - 2\cos(\gamma)} \\ &= -\sqrt{(\dot{\theta}_0)^2 + 2\cos(\theta_0 - \gamma) - 2\cos(\gamma)}. \end{aligned}$$

For the angular velocity at mid-stance to have a meaningful value, the term under the square root cannot have a non-zero value. Thus, we check

$$(\dot{\theta}_0)^2 > 2\cos(\gamma) - 2\cos(\theta_0 - \gamma). \quad (16)$$

*Computing period-one solutions:* Equation (13) represents a family of period-one solutions for the hip actuated simplest walker with three unknowns; namely,  $\gamma$ ,  $\dot{\theta}_0$ , and  $\theta_0$ . We assume values for two variables ( $\gamma$  and  $\dot{\theta}_0$ ), and solve for the third variable ( $\theta_0$ ), while ruling out solutions that violate (15) and (16).

#### D. Computing the feed-forward control $u_0$

The previous section assumes that the foot will be placed at a position  $\theta_0$  at the end of the step. This is our foot placement control. But we need to know what torque  $u_0$  in (2) will enable the desired foot placement.

We give one method to compute a time-based feed-forward torque  $u_0(t)$ . Our method for computing the feed-forward control law is based on the following observations: From (2), we see that the control law  $u_0$  can be found from the stance leg dynamics  $\theta(t)$  and the swing leg dynamics  $\phi(t)$ . The stance leg dynamics is decoupled from the swing leg dynamics and is completely known based on the foot placement control law presented in Sec. III-C. The swing leg dynamics can be determined by knowing the step time, the swing leg position at the beginning of swing phase, and end of swing phase.

The algorithm for computing  $u_0(t)$  follows:

(1) *Compute stance leg dynamics:* Compute and store values of stance leg rate  $\dot{\theta}(t)$ , by integrating (1) from initial state,  $\mathbf{q}_0^{\text{stance}} = \{\theta_0^+, \dot{\theta}_0^+\}$  from time  $t = 0$  to the step time  $t = t_{\text{step}}$ . A formula to compute the step time is given in Sec. III-E.

(2) *Compute swing leg dynamics:* We prescribe a third order polynomial of time to describe the swing leg motion. Thus we have,  $\phi(t) = a_0 + a_1t + a_2t^2 + a_3t^3$ , where  $a_0, a_1, a_2, a_3$  are constants that need to be determined. The constants can be found using the known values of the state at the beginning and end of single stance phase. The state at time  $t = 0$  for swing leg is  $\mathbf{q}_0^{\text{swing}} = \{2\theta_0^+, (1 - \cos 2\theta_0^+)\dot{\theta}_0^+\}$ . The state at time  $t = t_{\text{step}}$  is  $\mathbf{q}_f^{\text{swing}} = \{-2\theta_0^+, \dot{\phi}_{\text{swing}}^-\}$ , where  $\dot{\phi}_{\text{swing}}^-$  is a freely chosen swing leg velocity at foot-strike (more details on the how the choice of  $\dot{\phi}_{\text{swing}}^-$  affects the gait is given in Sec. IV-D). We get

$$\begin{aligned} a_0 &= 2\theta_0^+, \\ a_1 &= (1 - \cos 2\theta_0^+)\dot{\theta}_0^+, \\ a_2 &= \frac{-2(1 - \cos 2\theta_0^+)\dot{\theta}_0^+ - \dot{\phi}_{\text{swing}}^-}{t_{\text{step}}} - \frac{12\theta_0^+}{t_{\text{step}}^2}, \\ a_3 &= \frac{(1 - \cos 2\theta_0^+)\dot{\theta}_0^+ + \dot{\phi}_{\text{swing}}^-}{t_{\text{step}}^2} + \frac{8\theta_0^+}{t_{\text{step}}^3}. \end{aligned}$$

(3) *Computing  $u_0$ :* Given the swing leg motion  $\phi(t)$  and values of  $\dot{\theta}(t)$  in the previous two stages, and using (2) we compute the feed-forward control,

$$u_0(t) = \ddot{\phi}(t) - \sin(\theta(t) - \gamma) - \{\dot{\theta}^2(t) - \cos(\theta(t) - \gamma)\} \sin(\phi(t)).$$

To summarize, we need the values of  $\gamma$ ,  $\theta_0^+$ ,  $\dot{\theta}_0^+$ ,  $t_{\text{step}}$ , and  $\dot{\phi}_{\text{swing}}^-$  to compute the feed-forward torque  $u_0(t)$ .

#### E. Step time, Step length, and Step velocity

We obtain the non-dimensional values of the step time  $t_{\text{step}}$ , the step length  $d_{\text{step}}$  and the step velocity  $v_{\text{step}}$  using the formulae below.

$$\begin{aligned} t_{\text{step}} &= \int_{\theta^+}^{\theta^-} \frac{d\theta}{\dot{\theta}}, \\ &= \int_{\theta^+}^{-\theta^+} \frac{d\theta}{\sqrt{(\dot{\theta}^+)^2 + 2(\cos(\theta^+ - \gamma) - \cos(\theta - \gamma))}}, \\ &= \int_{\theta_0}^{-\theta_0} \frac{d\theta}{\sqrt{(\dot{\theta}_0)^2 + 2(\cos(\theta_0 - \gamma) - \cos(\theta - \gamma))}}, \end{aligned} \quad (17)$$

$$d_{\text{step}} = 2\sin(\theta_0), \quad (18)$$

$$v_{\text{step}} = \frac{d_{\text{step}}}{t_{\text{step}}}. \quad (19)$$

## IV. RESULTS

### A. Range of solutions

Fig. 2 shows a plot of the stance leg angle after foot-strike vs. non-dimensional stance leg rate after foot-strike for period-one walking obtained by solving (13). The grey area shows the region where there are feasible walking solutions for our model. We obtain the right edge of the feasible region by checking the condition given by (15), which is the condition for a zero ground reaction force. We obtain the left edge of the feasible region by checking the condition given by (16), which is the condition that the stance leg has sufficient velocity to make it to the top of the pendular arc.

We found walking solutions for slopes ranging from 0 to 15.42 degrees. For a given slope, there is family of period-one solutions that lies on the solid black line. In other words, for a given slope, if we choose a particular stance leg rate after foot-strike then we have a fixed stance leg angle after foot-strike for steady state walking and vice versa.

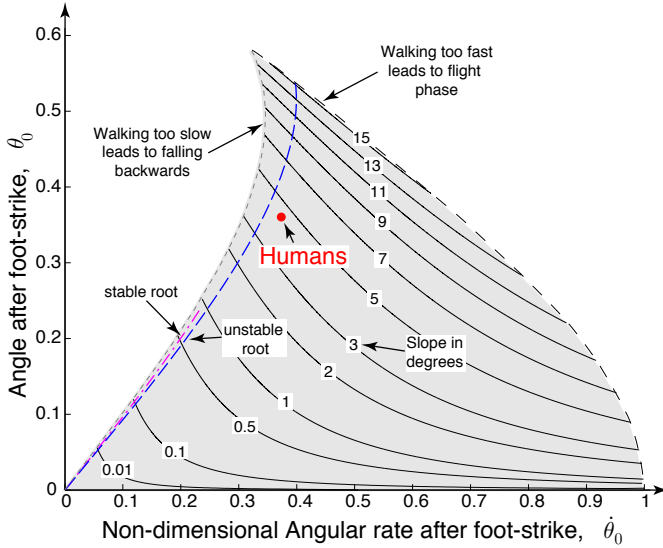


Fig. 2. Stance leg angle after foot-strike vs. non-dimensional stance leg rate after foot-strike for period-one walking. The grey area shows the feasible walking region.

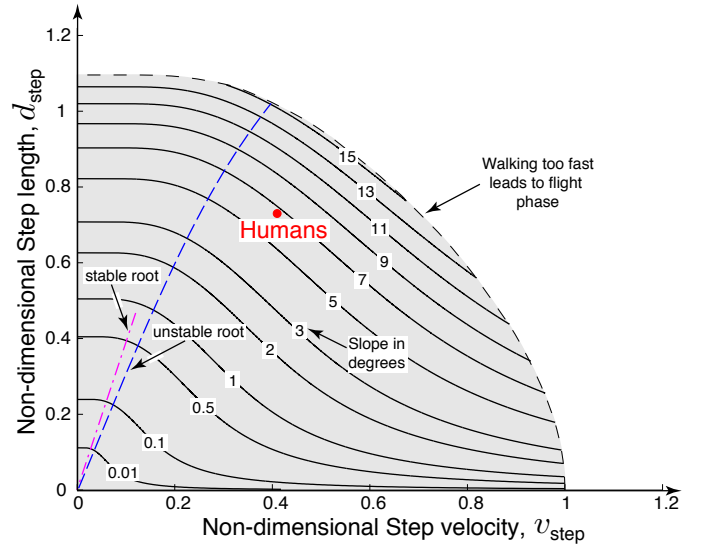


Fig. 4. Non-dimensional step length vs. non-dimensional step velocity. The grey area shows the feasible region of walking.

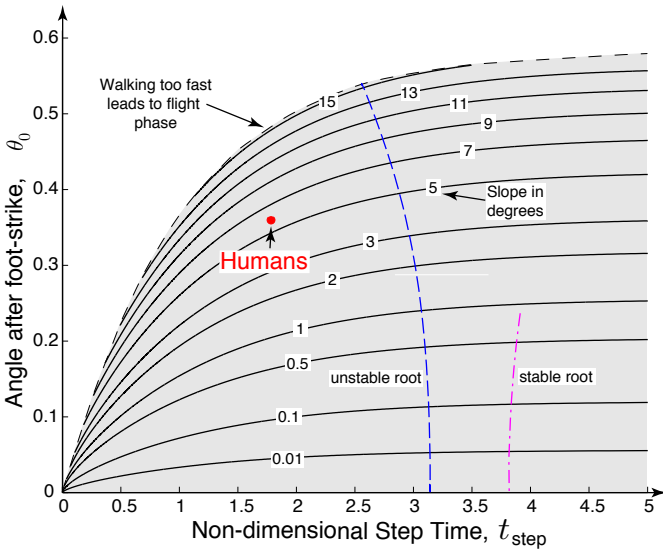


Fig. 3. Stance leg angle after foot-strike vs. non-dimensional step time for period-one walking. The grey area shows the feasible walking region.

We also plot the non-dimensional angle at foot-strike vs. the non-dimensional step time obtained from (17). This is shown in Fig. 3. Using (18) and (19), we plot the non-dimensional step length vs. non-dimensional step velocity, and is shown in Fig. 4.

### B. Passive solutions

Using analysis methods described in Section III-B, we found period-one solutions for the un-actuated slope walker. The solutions can be classified as stable or unstable solutions based on eigenvalues of the Jacobian of the Poincaré map,  $\mathcal{S}$ . The walking gait is stable if the biggest eigenvalue (after taking the norm) is smaller than 1 and unstable if it is greater than 1.

The stable solution (magenta dash dotted line) is obtained for a slope range of 0 to 0.87 degrees. The unstable solution (blue dashed line) is obtained for a slope range of 0 to 15.42 degrees, beyond

which there are solutions with a flight phase (ground reaction force on the stance leg goes to zero), and are ruled out. These results are in agreement with past results [2], [6]. We plot these passive solutions in Figs. 2 to 4.

### C. Average human walking

It is interesting to know at what slope our model is capable of walking at average human speed and stride length.

To compute nominal human walking speed and step length we did the following. We obtained the average human walking speed from reference [7] and is  $v = 1.3$  m/s. We non-dimensionalised the velocity by dividing with  $\sqrt{g\ell}$ , where gravity  $g \sim 10$  m/s<sup>2</sup> and average human leg length  $\ell = 1$  m. Thus,  $v_{\text{step}} = v/\sqrt{g\ell} = 1.3/\sqrt{10 \times 1} = 0.41$ . To get the non-dimensional step length, we use the empirical fit between step length and step velocity for average human walking from reference [8],  $d_{\text{step}} = 1.25 \times v_{\text{step}}^{0.6}$ . Putting  $v_{\text{step}} = 0.41$  gives,  $d_{\text{step}} = 1.25 \times 0.41^{0.6} = 0.73$ .

After plotting the average human values in Fig. 4, we found that average human steady state walking is possible for the simplest walker at a slope of 6.62 degrees.

Substituting the slope, and values for human speed and step length in formula given in Section III-E, we compute the stance leg angle after foot-strike,  $\theta_0^+ = 0.3604$ , the stance leg angular rate after foot-strike,  $\dot{\theta}_0^+ = 0.3736$ , and  $t_{\text{step}} = 1.7805$ . We plot these average human walking values in Figs. 2 and 3.

### D. Control law

To compute the feed-forward control law,  $u(t)$ , we follow the recipe given in Section III-D. For example, to generate the control law for walking at human speeds, we use the following values:  $\gamma = 6.62$  degrees,  $\theta_0^+ = 0.3604$ ,  $\dot{\theta}_0^+ = 0.3736$ ,  $t_{\text{step}} = 1.7805$ , while  $\dot{\phi}_{\text{swing}}^-$  can take any value.

Although the swing leg velocity at foot-strike,  $\dot{\phi}_{\text{swing}}^-$ , does not affect the gait planner, it does affect the stability. Wisse et al. [9] did extensive simulations to see the effect of swing leg velocity at foot-strike  $\dot{\phi}_{\text{swing}}^-$  using the same model we describe here. They found that a mild swing leg retraction, that is, a backward motion

of the swing leg with respect to the stance leg just before foot-strike improves walking stability. They also found that swing leg protraction (a forward motion of the swing leg with respect to the stance leg) is consistently unstable. Note that the stability is calculated by eigenvalues of the Poincaré map as described in Section III-B

## V. DISCUSSION

### A. Use of energy regulation between steps for gait planning

The essence of gait planning in this paper is to regulate energy between steps using foot placement. The robot gains potential energy every step as it descends down the slope. This excess energy needs to be dissipated to enable steady state walking. The foot placement control places the foot in such a way that the potential energy gained per step is exactly balanced by the energy lost during collision of the swing foot with the ground.

### B. Similarity with Hybrid Zero Dynamics and the rimless wheel

Our method of reducing the Poincaré return map to lower dimension using the actuated degrees of freedom is similar to the Hybrid Zero Dynamics (HZD) idea proposed by Grizzle et al. [10] and implemented on hardware by Westervelt et al. [11]. In HZD, the control law is such that the actuated degrees of freedom are functions of the un-actuated degrees of freedom. The net effect of such a control law reduces the Poincaré map to a dimension equal to the un-actuated degrees of freedom. So, for a 2 degree of freedom robot with 1 actuator, like the robot model presented here, the Poincaré map is of dimension  $2 - 1 = 1$ . However, HZD tries to enforce constraints throughout the walk cycle, while the foot placement controller presented here tries to enforce the constraint only at foot-strike.

The rimless wheel is another passive dynamic walking model that shows two families of period-one solutions for a range of slopes [12] just like the un-actuated simplest walker. In this case, the spoke angle is fixed. If we add an actuator to the rimless wheel that enables it to adjust the inter-spoke angle at every step, then the resulting model would be identical to the model presented here.

### C. Use of foot placement to control practical bipedal systems

Finally, we present some extensions to our model that will enable use of foot placement to control practical bipedal systems.

Our compass gait model has straight legs and hence foot scuffing during leg swing is inevitable. A simple extension would be to add a knee joint to the swing leg. By assuming a negligible mass at the thigh and shank as compared to the hip, it would be easy to extend the results of this paper. In this case, the swing leg dynamics during single stance phase will have dynamics of the knee and shank, and also a knee-strike besides a foot-strike. By adding an actuator to the knee joint and controlling it appropriately, it is possible to develop a controller that prevents foot scuffing. See Garcia et al. [13] for analysis of kneed passive dynamic walkers.

We have focussed on gait planning exclusively, but gait stability is important. One method of improving gait stability, is to do a swing leg retraction (swing leg moves backward before foot-strike), and has been discussed in the Sec. IV-D. Another method is to wrap a feedback controller on top of the feed-forward controller. The feedback controller serves to bring the system back to the nominal steady state gait in the event of a disturbance. For example, we have used an event-based feedback controller that tries to cancel the effect of disturbance in one step based on linearizing the Poincaré map [14].

One of the biggest limitation of this model is that it cannot sustain steady state walking on level ground. For the robot to walk on level

ground, the hip actuator needs to supply energy lost during foot-strike. However, as the swing leg dynamics are de-coupled with the stance leg dynamics, the hip actuator cannot supplying energy to the robot. One extension would be to add a telescopic actuator that provides an ankle push-off to power walking. For example, we have used a combination of ankle push-off and foot placement to do gait planning and control of the compass gait model [15]. Another idea would be to add an actuated torso [16].

## VI. CONCLUSIONS

In this paper, we shown how foot placement control in the simplest slope walker can lead to dramatic increase in the solution space over the un-actuated case. The central idea behind foot placement control is to balance the energy gained during descent with the energy lost during foot-strike. This method can be extended to practical bipedal robots by the following extensions: (1) Add a telescopic leg or an actuated torso to power walking and to realize walking on level ground. (2) Add knee joint to avoid foot scuffing. (3) Add a feedback controller that compensates for external disturbances.

## REFERENCES

- [1] T. McGeer, "Passive dynamic walking," *International Journal of Robotics Research*, vol. 9, no. 2, pp. 62–82, 1990.
- [2] M. Garcia, A. Chatterjee, A. Ruina, and M. Coleman, "The simplest walking model: Stability, complexity, and scaling," *ASME J. of Biomech. Eng.*, vol. 120, no. 2, pp. 281–288, 1998.
- [3] J. Pratt, J. Carff, S. Drakunov, and A. Goswami, "Capture point: A step toward humanoid push recovery," in *Humanoid Robots, 2006 6th IEEE-RAS International Conference on*. IEEE, 4-6 December 2006, Genova, Italy, pp. 200–207.
- [4] D. L. Wight, E. G. Kubica, and D. W. Wang, "Introduction of the foot placement estimator: A dynamic measure of balance for bipedal robotics," *Journal of Computational and Nonlinear Dynamics*, vol. 3, no. 1, pp. 011009–1:10, 2008.
- [5] S. Strogatz, *Nonlinear dynamics and chaos: with applications to physics, biology, chemistry and engineering*. Perseus Books Group, 2001.
- [6] P. A. Bhounsule, "Numerical accuracy of two benchmark models of walking: the rimless wheel and the simplest walker," *Dynamics of Continuous, Discrete and Impulsive Systems Series B: Application and Algorithms*, 2014 (in press).
- [7] H. J. Ralston, "Energy-speed relation and optimal speed during level walking," *Internationale Zeitschrift für angewandte Physiologie einschließlich Arbeitsphysiologie*, vol. 17, no. 4, pp. 277–283, 1958.
- [8] R. Alexander and G. Maloiy, "Stride lengths and stride frequencies of primates," *Journal of Zoology*, vol. 202, no. 4, pp. 577–582, 1984.
- [9] M. Wisse, C. G. Atkeson, and D. K. Kloimwieder, "Swing leg retraction helps biped walking stability," in *Humanoid Robots, 2005 5th IEEE-RAS International Conference on*. IEEE, 5-7 December 2005, Tsukuba, Japan, pp. 295–300.
- [10] J. W. Grizzle, G. Abba, and F. Plestan, "Asymptotically stable walking for biped robots: Analysis via systems with impulse effects," *Automatic Control, IEEE Transactions on*, vol. 46, no. 1, pp. 51–64, 2001.
- [11] E. R. Westervelt, J. W. Grizzle, and D. E. Koditschek, "Hybrid zero dynamics of planar biped walkers," *Automatic Control, IEEE Transactions on*, vol. 48, no. 1, pp. 42–56, 2003.
- [12] M. Coleman, "A stability study of a three-dimensional passive-dynamic model of human gait," Ph.D. dissertation, Cornell University, 1998.
- [13] M. Garcia, A. Chatterjee, and A. Ruina, "Efficiency, speed, and scaling of two-dimensional passive-dynamic walking," *Dynamics and Stability of Systems*, vol. 15, no. 2, pp. 75–99, 2000.
- [14] P. Bhounsule, J. Cortell, A. Grewal, B. Hendriksen, J. Karsen, C. Paul, and A. Ruina, "Low-bandwidth reflex-based control for lower power walking: 65 km on a single battery charge," *Intl. Journal of Robotics Research*, 2014 (in press).
- [15] P. A. Bhounsule, "Control of a compass gait walker based on energy regulation using ankle push-off and foot placement," *Robotica*, vol. FirstView, pp. 1–11, May 2014. [Online]. Available: [http://journals.cambridge.org/article\\_S0263574714000745](http://journals.cambridge.org/article_S0263574714000745)
- [16] T. Narukawa, M. Takahashi, and K. Yoshida, "Efficient walking with optimization for a planar biped walker with a torso by hip actuators and springs," *Robotica*, vol. 29, no. 4, pp. 641–648, 2011.